Bio-inspired Dynamic Gradients Regulated by Supramolecular Bindings in Receptor-Embedded Hydrogel Matrices

Xinglong Luan,[a] Yihe Zhang,*[a] Jing Wu,[b] Pascal Jonkheijm,[c] Guangtao Li,[d] Lei Jiang,[e] Jurriaan Huskens,*[c] and Qi An*[a]

The kinetics of supramolecular bindings are fundamentally important for molecular motions and spatial–temporal distributions in biological systems, but have rarely been employed in preparing artificial materials. This report proposes a bio-inspired concept to regulate dynamic gradients through the coupled supramolecular binding and diffusion process in receptor-embedded hydrogel matrices. A new type of hydrogel that uses cyclodextrin (CD) as both the gelling moiety and the receptors is prepared as the diffusion matrices. The diffusible guest, 4-aminoazobenzene, quickly and reversibly binds to ma-trices-bound CD during diffusion and generates steeper gradients than regular diffusion. Weakened bindings induced through UV irradiation extend the gradients. Combined with numerical simulation, these results indicate that the coupled binding–diffusion could be viewed as slowed diffusion, regulated jointly by the binding constant and the equilibrium receptor concentrations, and gradients within a bio-relevant extent of 4 mm are preserved up to 90 h. This report should inspire design strategies of biomedical or cell-culturing materials.

1. Introduction

Regulated spatial–temporal distributions of various bioactive factors are characteristic of biological complexity.[1] Dynamic spatial concentration gradients are the most frequently observed spatial–temporal distribution phenomena in biological systems and are indispensable in various biological functionalities.[2–5] However, integrating biomimetic concentration gradi-

[a] X. Luan, Prof. Dr. Y. Zhang, Dr. Q. An
Beijing Key Laboratory of Materials Utilization of Nonmetallic Minerals and Solid Wastes, National Laboratory of Mineral Materials
School of Materials Science and Technology
China University of Geosciences, Beijing 100083 (P. R. China)
E-mail: an@cugb.edu.cn
        zyh@cugb.edu.cn

[b] Dr. J. Wu
School of Science, China University of Geosciences
Beijing 100083 (P. R. China)

[c] Prof. Dr. P. Jonkheijm, Prof. Dr. J. Huskens
Molecular Nanofabrication Group
MESA + Institute of Nanotechnology, University of Twente
7500 AE Enschede (The Netherlands)
E-mail: J.Huskens@utwente.nl

[d] Prof. Dr. G. Li
Department of Chemistry, Tsinghua University
Beijing 100084 (P. R. China)

[e] Prof. Dr. L. Jiang
Institute of Chemistry, Chinese Academy of Sciences
Beijing 100084 (P. R. China)

ents in artificial matrices with corresponding length scales (hundreds of micrometers to several millimeters) has remained a persisting challenge.[6] Photolithography, dip-coating, and printing can prepare only static gradients.[7,8] Microfluidic devices or electrochemical reactions can generate dynamic spatial concentration gradients, but require external disturbing energies (electric potential or pressure, etc.).[9–12] By clear contrast, within biological systems, gradients are generated and diminished extremely efficiently in a component-specific manner, using only chemical energies.[2,13] Several lines of evidence strongly support the notion that supramolecular bindings in the process of diffusion play important roles in gradient formation and regulation; the gradient-forming factors (morphogens) simultaneously diffuse[14,15] and reversibly bind to matrices-bound receptors,[16–18] and the coupled "supramolecular binding–diffusion" process, in turn, regulates dynamic gradients of the active factors.[2,14] These observations prompt us to ask whether integrating supramolecular bindings in diffusion processes would regulate spatial–temporal concentration gradients in artificial materials.

Inspired by biological phenomena, we demonstrate here a novel concept to regulate dynamic chemical gradients in receptor-embedded hydrogel matrices through the combined processes of supramolecular bindings and diffusion (Figure 1). The concentration gradients of a diffusive guest (4-aminoazobenzene) in the bio-relevant extent of hundreds of micrometers to several millimeters are formed in a hydrogel-filled channel when 4-aminoazobenzene diffuses through the matrices. During diffusion, 4-aminoazobenzene quickly and reversibly binds to the matrices-bound receptor cyclodextrin (CD). Dynamic diffusing gradients formed through this coupled bind-
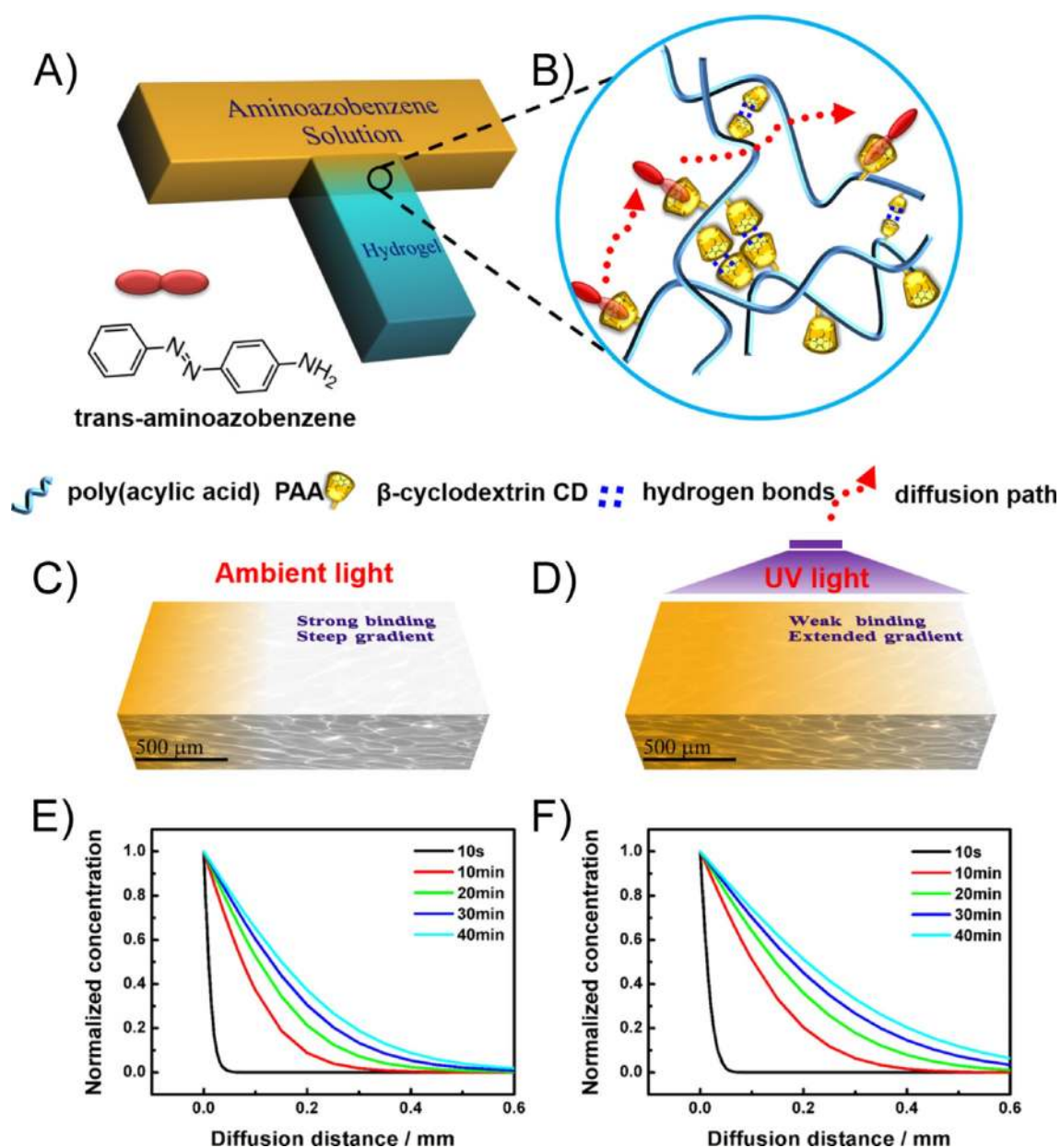
Figure 1. A) Schematic display of the diffusion setup: a T-shaped fluidic channel with a channel width of 2 mm and depth of 500 μm, within which the spatial temporal gradients are generated. The perpendicularly oriented channels are respectively filled with PAA-CD hydrogel and a solution of 4-aminoazobenzene. B) When 4-aminoazobenzene diffuses into the hydrogel matrices, it quickly and reversibly binds to matrices-bound receptors, CD. Schematic concentration gradients of 4-aminoazobenzene at $t = 40$ min C) under ambient light and D) under 365 nm light irradiation. Simulated concentration profiles E) under ambient light and F) under 365 nm light irradiation.

ing–diffusion process are remarkably steeper than those formed through regular diffusion processes. Weakened bindings induced by the isomerization of 4-aminoazobenzene, using 365 nm light irradiation, extended the length of the gradients. To elucidate the mechanism underlining the binding-regulated gradients, we propose a mathematical expression to state the relationship between the apparent diffusion coefficient and the supramolecular binding parameters, which indicates that coupled binding–diffusion could be viewed as slowed diffusion, regulated jointly by the equilibrium receptor concentration and the binding constant. Numerical simulation

verified that the spatial–temporal molecular distributions in the coupled binding–diffusion processes could be described by using Fick's diffusion law when employing the apparent diffusion coefficient. In addition, the restrained diffusion could relate to the phenomena of spatial molecular reservations and acute concentration drops in adjacent areas of the matrices. A key novelty achieved here by the binding-regulated diffusing gradients is that the kinetics of supramolecular bindings, instead of external energies, are used in regulating dynamic pattern formations. We expect this report to promote the application of the kinetics aspect of supramolecular bindings in the

regulation of spatial–temporal molecular distributions in artificial materials and inspire design strategies of biomedical materials.

2. Results and Discussion

We designed a new type of receptor-embedded hydrogel as the diffusion matrices. The hydrogel was composed of CD-grafted poly(acrylic acid) (PAA-CD, Scheme S1), which gelled by forming hydrogen bonds between CD moieties (Figure S1). Here, CD served dual roles, as the gel-formation moiety and the binding receptors. PAA-CD hydrogel formed in phosphate-buffered saline (PBS) over a wide range of polymer concentrations and CD grafting ratios (polymer concentration ca. 6.0–10.0 wt%, molarity grafting ratios above 4.3% at 6.0 wt% and

above 1.5% at 10.0 wt%, and combinations outside this concentration range were not studied), as shown in the gelling phase diagram in Figure 2A. The hydrogel was shear-thinning, which is a typical characteristic of supramolecular hydrogels,[19,20] and was injectable by using a syringe (Figure 2B). Serial rheological measurements indicated that the hydrogel presented shearing-thinning properties and the storage moduli were larger than loss moduli throughout the oscillation frequency range of 0.1–10 Hz. (Figure 2C,D), verifying that hydrogels were formed. As shown in Figure 2E, the viscosities and moduli strongly correlated with CD grafting ratios when the polymer concentration was 8.0 wt%; the solution viscosity remained unchanged when the CD grafting ratios were below 1.9%, whereas above a CD grafting ratio of 1.9%, the viscosities increased remarkably with grafting ratios from 50 Pa·s (at
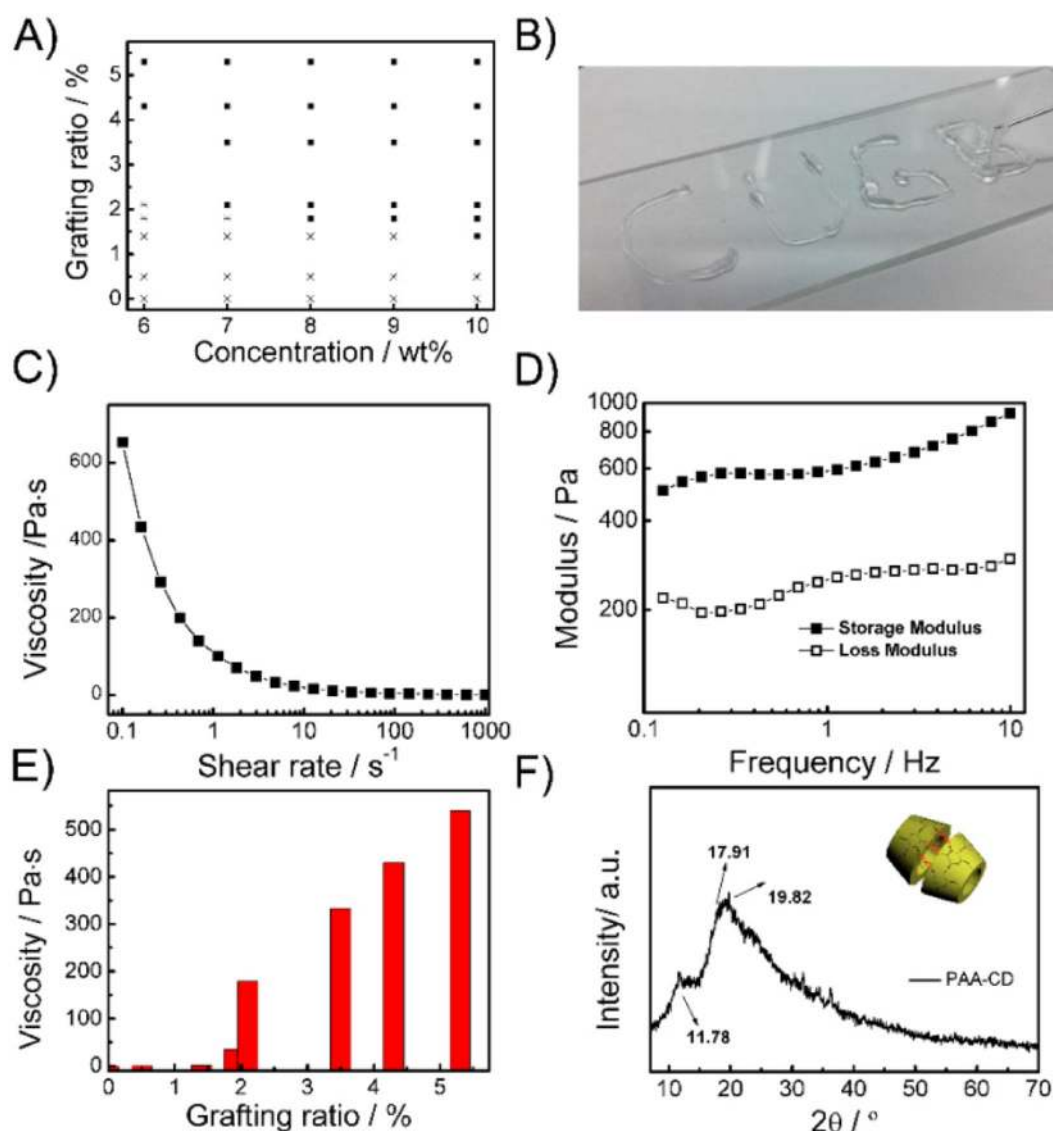

Figure 2. A) The gelling phase diagram of PAA-CD hydrogel: gelling is jointly determined by polymer concentrations and grafting ratios (solid square: hydrogel; star, solution or sol). B) Digital image of PAA-CD hydrogel injected from a syringe to form the pattern of CUGB (initials of the authors' institute; polymer concentration 8.0 wt%, grafting ratio 3.5%).C) Viscosities and D) moduli of PAA-CD hydrogel at a concentration of 8.0 wt% with a grafting ratio 5.3%.The black dots denote experimental data and black lines are guide to the eyes. E) Viscosities of PAA-CD hydrogel at a concentration of 8.0 wt% and a shearing rate of 0.1 s^{-1} with varying grafting ratios. F) XRD patterns of lyophilized PAA-CD hydrogel, which indicates the presence of head-to-head channel-type CD aggregates, as illustrated in the schematic inset.

grafting ratio 1.9%) to 540 Pa·s (at grafting ratio 5.3%). Moduli varied between 20 and 500 Pa versus grafting ratios, following a similar trend to the viscosities and presenting a clear critical point at a grafting ratio 1.9% (Figure S2). The existence of the critical gelling point is consistent with supramolecular multivalence theory, which states that multiple supramolecular interactions are addable only when the effective molarities (EMs) of the intermolecular binding moieties are above a critical value, and that the EM equals $1/K$ ($K =$ binding constant).[21, 22] The critical gelling EM of CD was calculated as 1.53×10^{-2} M, giving a binding constant between CDs of 65.4 M^{-1}, as detailed in the Supporting Information.

Notably, although interactions between CDs were remarkably weaker than the host–guest bindings between CDs/cucurbit[n]urils and their guests (which are typically larger than 1000 M^{-1}), the hydrogels formed in this study, upon a proper choice of grafting density and concentration, could present comparable moduli to those formed by using host–guest supramolecular pairs as physical cross linkages.[20] The as-prepared PAA-CD hydrogel displayed increasing viscosity and moduli at increasing pH values between pH 3 and 9 (Figures S3 and S4). These phenomena are consistent with a previous report that showed that enhanced ionization degrees of PAA caused expansion of polymer chains and increased gel viscosities and moduli.[23] Thus, all PAA-CD hydrogels used in the following sessions were prepared by using PBS (0.5 M) at pH 7.4 to ensure consistent rheological performance.

Hydrogel structural information probed by using XRD and ^{1}H NMR spectroscopy at varying temperatures further corroborated the notion that CD aggregates were responsible for hydrogel formation. Lyophilized hydrogel powders presented broad diffraction peaks at 11.78, 17.91, and 19.82° in the XRD patterns, as shown in Figure 2F. As observed before, these

peaks were generated by head-to-head channel-type CD aggregates held together through hydrogen bonds.[24] XRD patterns indicated that CD aggregates served as physical cross linkages in our hydrogel. Accordingly, ^{1}H NMR spectra of the PAA-CD hydrogel displayed no signals at 25°C, but presented characteristic PAA-CD signals at 60°C (Figure S5). At 60°C, the hydrogen bonds were broken and PAA-CD polymers were freed for rotation to give an NMR signal.[25] The interesting phenomenon worth mentioning was that only PAA-CD synthesized in aqueous solution was able to generate hydrogels. PAA-CD synthesized in DMF did not gel, despite the fact that grafting ratios of CD were high (up to 4.7%, data not shown). This was explained by a previous report, in which dipole organic solvents could irreversibly 'quench' the ability of CDs to form hydrogen bonds.[26] This evidence also explained why PAA-CD synthesized in organic solvent in a previous report did not gel without guest polymers.[27, 28]

A relative question when using PAA-CD hydrogel as the diffusion matrices is how the hydrogel would respond to the addition of the guest molecule 4-aminoazobenzene. As shown in Figures 3 and S6. The addition of 4-aminoazobenzene decreased hydrogel viscosities and moduli, but the mixture still presented larger storage modulus (G') than loss modulus (G'') values. 4-Aminoazobenzene was bound to CD cavities and shifted the equilibrium of the free-CD moiety versus CD aggregates in PAA-CD hydrogels, and decreased the number of CD aggregates.[29] As a result, the viscosities of PAA-CD hydrogel decreased from 540 to 120 Pa·s when the molarity ratio of 4-aminoazobenzene/CD increased from 0 to 0.8. 4-Aminoazobenzene was isomerized with 365 nm irradiation, which decreased its binding constant towards CD.[30, 31] In response to the weakened binding, more CD aggregates were formed, and hydrogel rheology was partially restored and the once-flowing mixture
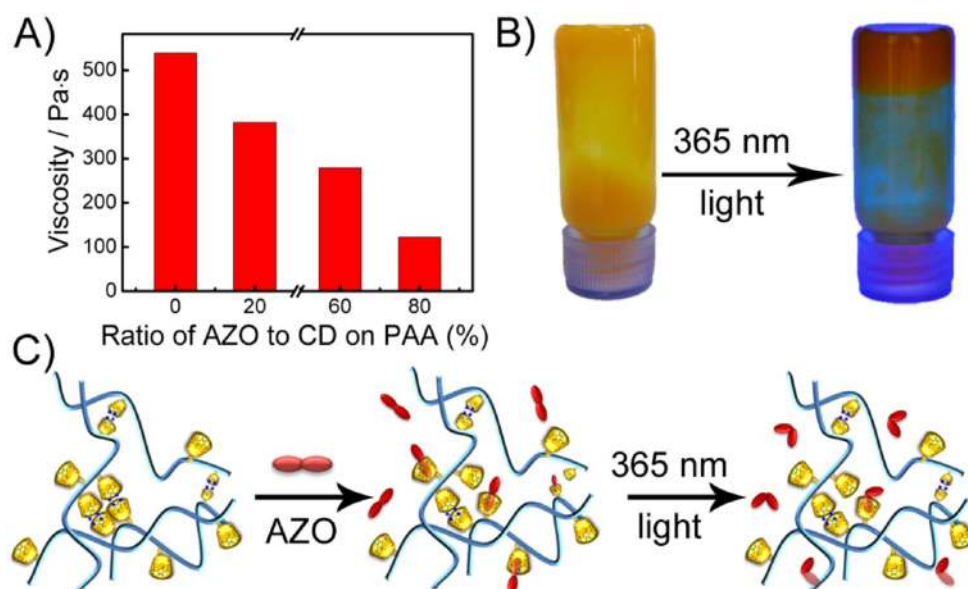

Figure 3. A) Viscosities of PAA-CD hydrogel (8.0 wt%, grafting ratio 5.3%) with varying amount of loaded 4-aminoazobenzene. B) The once-flowing, guest-loaded PAA-CD hydrogel is able to adhere to the upper part of a vial after 365 nm light irradiation, indicating the viscosities of the hydrogel increase after 365 nm light irradiation. C) Schematic illustration of the notion that the loading of 4-aminoazobenzene breaks hydrogen bonds between CDs, and after 365 nm light irradiation the CD aggregates increase.

was able to stay in the upper part of the vial after 365 nm light irradiation, as shown in Figures 3 B and 3 C.

The diffusion experiments were conducted in T-shaped fluidic channels, as shown in Figures 1 B and 4. PAA-CD hydrogel (concentration 8.0 wt%, grafting ratio 3.5%, CD moiety molarity 25.2 mM) was injected into the rectangular channel and a solution of 4-aminoazobenzene (2.1 mM) was introduced through the perpendicular channel. 4-Amionazobenzene diffused into PAA-CD hydrogel from the hydrogel channel entrance and reversibly bound to CD receptors during diffusion. Figure 4 A displays a typical selection of images during diffusion. To demonstrate that binding constants influence diffusing gradients in this coupled binding–diffusion process, a parallel set of experiments were conducted under 365 nm light irradiation, and the representative images obtained during diffusion are presented in Figure 4 B. These images indicated that the diffusion frontiers proceeded slower when diffusion was coupled with strong bindings (under ambient light). The dislocation of the diffusion frontier within 40 min was approximately 300 μm for diffusions under ambient light (strong binding), in comparison with 500 μm under 365 nm light (weak binding). This compari-

son indicated that supramolecular binding constants strongly influence the diffusing patterns (channel surface temperature raised by only 2 °C during 365 nm light irradiation, and this temperature rise did not influence diffusion). Pixel analysis of the images displayed in Figures 4 C and 4 D showed that stronger bindings resulted in steeper gradients. In other words, when stronger bindings to matrices-bound receptors exist in diffusion, a local rise in diffusive guest concentration imposed more spatially restrained influence, resulting in acute concentration decreases in adjacent areas, and the concentrated guests were effectively stopped from diffusing away. In comparison, weakened bindings during diffusion allowed the guests to reach areas further away in a specific amount of time.

The mechanism underlining binding-regulated diffusion was elucidated through mathematical reduction. We propose that the diffusion behaviors are regulated by intermolecular bindings through Equation (1); see also details and relative mass transport considerations[31] in the Supporting Information:

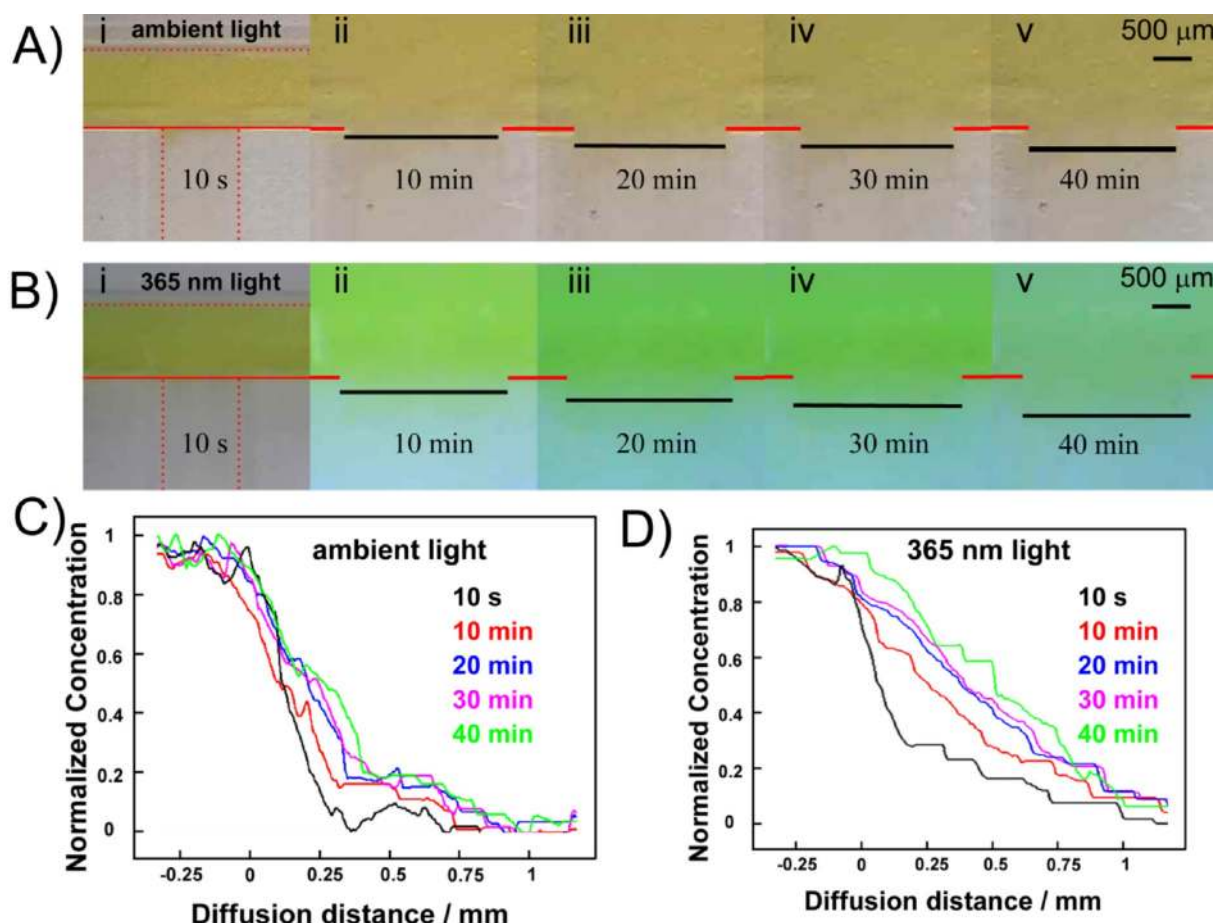$$Da = D_0 \cdot (K_a \cdot C + 1)^{-1} \tag{1}$$

Figure 4. Selected sets of images for the coupled binding–diffusion under A) ambient light and B) 365 nm light, indicating that diffusive frontier proceeded farther under 365 nm irradiation than that under ambient light. The yellow color is intrinsic of the diffusive molecule, 4-aminoazobenzene. The red and black lines are guide to the eyes; the dashed red lines sketch out the channel outlines, the solid red lines indicate the lower boundaries of the horizontal channel (x = 0 in diffusion), and the black lines indicate the diffusion frontiers. Diffusive spatial temporal profiles under C) ambient light and D) 365 nm light, derived through pixel analysis of the images in (A) and (B) using Image-J.

where D_a is the apparent diffusion coefficient in the coupled binding–diffusion process, D_0 the regular diffusion coefficient, and K_a the binding constant between 4-aminoazobenzen and CD of the unoccupied receptors. This mathematical expression clearly states that the coupled binding–diffusion processes can be viewed as slowed diffusions (as verified below).[33] Fast reversible intermolecular bindings decrease the diffusion coefficient, and the product of the binding constant and the equilibrium concentration of unoccupied receptors determines the significance of the influence. In our diffusion matrices, the equilibrium concentration of unoccupied CD was calculated to be 1.06×10^{-2} M, and was assumed to be constant throughout the diffusion areas (the assumption was made based on calculations, as detailed in the Supporting Information). According to Equation (1), D_a of *trans*-aminoazobenzene was calculated as 1.0×10^{-11} m^{2}s^{-1}, whereas that of *cis*-aminoazobenzene was 5.0×10^{-11} m^{2}s^{-1}.

The regulated diffusion, in turn, dictated spatial–temporal distributions of the diffusive molecule. The molecular spatial–temporal distributions were simulated by following Fick's diffusion law, using both Excel and a finite element model; the calculated apparent diffusion coefficient, D_a, was used in the simulation (as detailed in the Supporting Information). Simulation results indicated that, compared with regular diffusion ($D_0 = 1.0\times10^{-10}$ m^{2}s^{-1}), the binding between CD and 4-aminoazobenzene remarkably constrained molecular spatial distributions (Figures 1E, 1F, and 5A). The calculated dislocations of each selected concentration between 10 and 40 min were compared with those measured from experimental results under ambient light. The dislocations between 10 and 40 min were analyzed to avoid the instabilities at the beginning of the diffusion, and normalized concentrations between 0.4 and 0.8 were

analyzed, owing to the image resolutions. The comparisons indicated that Fick's diffusion law satisfactorily captures the concentration distribution characteristics in the coupled binding–diffusion process. Although closer observation over the comparison results revealed that binding–diffusion in PAA-CD hydrogel presented a slight "super-diffusion" phenomenon for high concentrations (normalized concentration of 0.7 and 0.8) in experimental observations, the high concentrations proceeded slightly faster than dictated by Fick's diffusion law (less than 25% disparities in diffusing distances, small enough to fall within the error regions, but large enough to observe). The observed super-diffusion phenomena were attributed to the guest-responsive nature of the PAA-CD hydrogel. Higher guest concentrations led to decreases in the local matrices rheology and local equilibrium concentrations of unoccupied receptors, and these two factors together resulted in a slight increase in the diffusion speed. In addition, simulation for longer time spans, shown in Figures 5B, 5C, and S7 indicated that, when coupled with strong binding ($D_a = 1.0\times10^{-11}$ m^{2}s^{-1}), diffusing gradients within a bio-relevant extent of 4 mm could be preserved for up to 90 h. In comparison, when diffusions were coupled with weak binding ($D_a = 5.0\times10^{-11}$ m^{2}s^{-1}) or for regular diffusion ($D_0 = 1.0\times10^{-10}$ m^{2}s^{-1}), gradients were diminished at 90 h in the millimeter scale, owing to diffusions taking place. As spatial concentration gradients of bioactive factors for 48–96 h are frequently observed in biological systems, the well-preserved gradients for up to 90 h in our receptor-rich matrices suggest that this proposed gradient-generation strategy is potentially applicable in tissue engineering or cell-culturing materials. The regulated diffusions should also be applicable in the design of biomedical materials, such as in controlled-release devices.
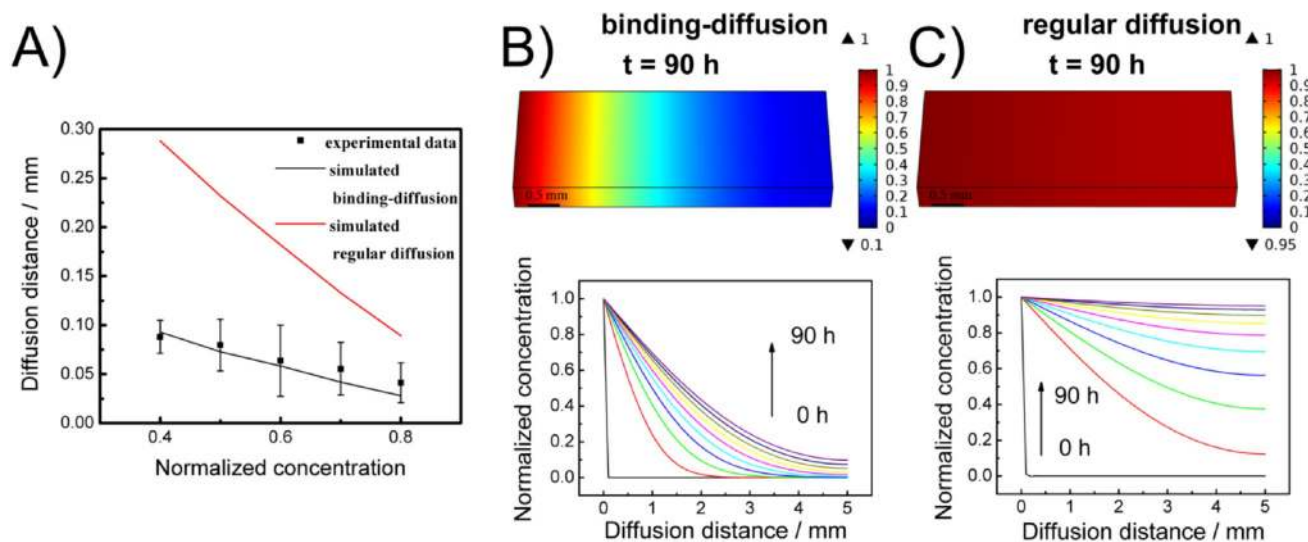

Figure 5. A) Comparison of the dislocation of each particular concentration in the regular diffusions (the red line, simulated by using $D_0 = 1.0\times10^{-10}$ m^{2}s^{-1}) and in the coupled binding–diffusion experiments (black squares, experimental data under ambient light with error bars generated from eight separate experiments; black line, simulated using Excel simulation, as detailed in Section 11 of the Supporting Information). B) Simulated concentration distributions for the coupled binding–diffusion of *trans*-aminoazobenzene at $t = 90$ h (upper) and the corresponding concentration spatial–temporal profiles through 0–90 h at a time interval of 10 h (lower). C) Simulated concentration distribution for regular diffusion with D_0 at $t = 90$ h (upper) and the corresponding concentration spatial–temporal profiles through 0–90 h at a time interval of 10 h (lower).

3. Conclusions

We have proposed a bio-inspired concept to regulate dynamic concentration gradients in hydrogel matrices by coupling fast reversible intermolecular bindings in diffusion. We have shown that fast reversible bindings of the diffusive molecules to matrices-bound receptors decreased the molecular diffusion coefficient, and the binding constant and equilibrium receptor concentrations jointly determine the extent of the retardation of diffusion. The resultant molecular spatial–temporal distribution could be described by using Fick's diffusion law. The restrained diffusion relates to the phenomena of spatial molecular reservations and concentration disparities in adjacent areas in the matrices, which have been frequently observed in biological systems. As the coupled binding–diffusion phenomena are omnipresent in biological systems, but have remained insufficiently understood, we expect our findings not only to provide new insights into the kinetics of supramolecular bindings that could be used in engineering spatial–temporal patterns in artificial materials, but also to provide an artificial platform that assists the development of a deeper scientific understanding of coupled supramolecular bindings and diffusions in biological contexts.

Experimental Section

Preparation of PAA-CD Polymer and Hydrogel

In a typical synthesis, 400 mg PAA (5.56 mM acrylic acid unit) was dissolved in 30 mL PBS (pH 7.4). To this solution, 1-ethyl-3-(3-dimethylaminopropyl) carbodiimide (EDC) (2 equiv of acrylic acid unit) and N-Hydroxysuccinimide (NHS) (2 equiv of acrylic acid unit) were added. After stirring for about 2 h, 6-mono-amino-6-mono-deoxy-β-CD (0.1 equiv of acrylic acid unit) was added, and the solution was stirred for 48 h at room temperature. Then, the solution was transferred to a dialytic bag and dialyzed for 5 days. After dialysis, PAA-CD was obtained by freeze-drying. By varying the feed ratios of amino-CD to PAA, PAA-CD polymers with different grafting ratios were obtained, and the grafting ratios were quantified by using ^{1}H NMR spectroscopy. The lyophilized powder of PAA-CD was used to prepare solutions or hydrogels at required concentrations in 0.05 M PBS (pH 7.4). At appropriate concentrations, PAA-CD gels spontaneously formed in PBS after stirring.

^{1}H NMR (400 MHz, D$_2$O): $\delta = 1.55$–2.05 [CH2 (pAA)], 2.24–2.60 [CH (pAA)], 3.51–3.78 [C2,4 H (CD)], 3.79–4.07 [C3,5,6 H (CD)], 5.02–5.17 ppm [C1 H (CD)].

Generation of the Gelling Phase Diagram of PAA-CD

The sol-gel transition area (grafting ratios within the range 1.5–3.5% throughout concentration ranges from 6 to 10 wt%, plus grafting ratio 4.3% for 6 wt%) was determined by using rheological measurements. Samples with storage moduli larger than loss moduli were labeled as gels. Outside the transition area, gelation was determined through phenomena observation.

Observations of Diffusion in Fluidic Channels under Ambient Light and 365 nm Light

Diffusions in channels were conducted in T-shaped fluidic channels (cross section 500 μm×2 mm). The hydrogel with a grafting ratio of 3.5% and concentration of 8 wt% was injected in one channel. Then, the perpendicular channel was washed with deionized water and dried by using nitrogen. Afterwards, a solution of 4-aminoazobenzene (2.07 mM) was introduced into the dried channel. Ambient light from a white LED lamp array was used to observe and record the diffusion processes.

Diffusions under 365 nm (20 W from a distance of 5 cm) light was conducted in an identical channel. 365 nm irradiation was continuously applied throughout the diffusion process to keep (the majority of) 4-aminoazobenzene as *cis*-isomers. The ambient light remained in the background to obtain a bright enough view to record and observe the diffusion process. During 365 nm light irradiation, the surface temperature of the diffusion setup increased by 2 °C. The influence of the temperature rise on diffusion speeds was negligible.

[1] P. J. Keller, *Science* **2013**, *340*, 1234168.
[2] E. Bier, E. M. De Robertis, *Science* **2015**, *348*, aaa5838.
[3] S. Shimozono, T. Iimura, T. Kitaguchi, S. Higashijima, A. Miyawaki, *Nature* **2013**, *496*, 363.
[4] E. Donà, J. D. Barry, G. Valentin, C. Quirin, A. Khmelinskii, A. Kunze, S. Durdu, L. R. Newton, A. Fernandez-Minan, W. Huber, M. Knop, D. Gilmour, *Nature* **2013**, *503*, 285.
[5] M. Weber, R. Hauschild, J. Schwarz, C. Moussion, I. de Vries, D. F. Legler, S. A. Luther, T. Bollenbach, M. Sixt, *Science* **2013**, *339*, 328.
[6] J. D. Wu, Z. W. Mao, H. P. Tan, L. L. Han, T. C. Ren, C. Y. Gao, *Interface Focus* **2012**, *2*, 337.
[7] J. Genzer, R. R. Bhat, *Langmuir* **2008**, *24*, 2294.
[8] X. K. Lin, Q. He, J. B. Li, *Chem. Soc. Rev.* **2012**, *41*, 3584.
[9] V. Sivagnanam, M. A. M. Gijs, *Chem. Rev.* **2013**, *113*, 3214.
[10] S. O. Krabbenborg, J. Huskens, *Angew. Chem. Int. Ed.* **2014**, *53*, 9152; *Angew. Chem.* **2014**, *126*, 9304.
[11] S. Kim, H. J. Kim, N. L. Jeon, *Integr. Biol.* **2010**, *2*, 584.
[12] S. O. Krabbenborg, C. Nicosia, P. K. Chen, J. Huskens, *Nat. Commun.* **2013**, *4*, 1667.
[13] K. W. Rogers, A. F. Schier, *Annu. Rev. Cell Biol.* **2011**, *27*, 377.
[14] S. R. Yu, M. Burkhardt, M. Nowak, J. Ries, Z. Petrasek, S. Scholpp, P. Schwille, M. Brand, *Nature* **2009**, *461*, 533.
[15] S. H. Zhou, W. C. Lo, J. L. Suhalim, M. A. Digman, E. Gratton, Q. Nie, A. D. Lander, *Curr. Biol.* **2012**, *22*, 668.
[16] K. D. Schleicher, S. L. Dettmer, L. E. Kapinos, S. Pagliara, U. F. Keyser, S. Jeney, R. Y. H. Lim, *Nat. Nanotechnol.* **2014**, *9*, 525.
[17] J. Huskens, *Nat. Nanotechnol.* **2014**, *9*, 500.
[18] R. G. Thorne, A. Lakkaraju, E. Rodriguez-Boulan, C. Nicholson, *Proc. Natl. Acad. Sci. USA* **2008**, *105*, 8416.
[19] M. Guvendiren, H. D. Lu, J. A. Burdick, *Soft Matter* **2012**, *8*, 260.
[20] E. A. Appel, F. Biedermann, U. Rauwald, S. T. Jones, J. M. Zayed, O. A. Scherman, *J. Am. Chem. Soc.* **2010**, *132*, 14251.

[21] J. Huskens, A. Mulder, T. Auletta, C. A. Nijhuis, M. J. W. Ludden, D. N. Reinhoudt, *J. Am. Chem. Soc.* **2004**, *126*, 6784.

[22] A. Mulder, T. Auletta, A. Sartori, S. Del Ciotto, A. Casnati, R. Ungaro, J. Huskens, D. N. Reinhoudt, *J. Am. Chem. Soc.* **2004**, *126*, 6627.

[23] J. Byeongmoon, W. K. Sung, H. B. You, *Adv. Drug Delivery Rev.* **2002**, *54*, 37.

[24] Y. F. He, X. H. Shen, Q. D. Chen, H. C. Gao, *Phys. Chem. Chem. Phys.* **2011**, *13*, 447.

[25] C. Travelet, G. Schlatter, P. Hebraud, C. Brochon, A. Lapp, G. Hadziioan-nou, *Langmuir* **2009**, *25*, 8723.

[26] Y. Marui, A. Kikuzawa, T. Kida, M. Akashi, *Langmuir* **2010**, *26*, 11441.

[27] I. Tomatsu, A. Hashidzume, A. Harada, *J. Am. Chem. Soc.* **2006**, *128*, 2226.

[28] D. Wang, M. Wagner, H.-J. Butt, S. Wu, *Soft Matter* **2015**, *11*, 7656.

[29] Y. Liu, Y. L. Zhao, Y. Chen, D. S. Guo, *Org. Biomol. Chem.* **2005**, *3*, 584.

[30] A. Beharry, G. A. Woolley, *Chem. Soc. Rev.* **2011**, *40*, 4422.

[31] J. A. Krings, B. Vonhoren, P. Tegeder, V. Siozios, M. Peterlechner, B. J. Ravoo, *J. Mater. Chem. A* **2014**, *2*, 9587.

[32] A. Perl, G. Casado, D. Thompson, H. H. Dam, P. Jonkheijm, D. N. Reinhoudt, J. Huskens, *Nat. Chem.* **2011**, *3*, 317.

[33] N. Lorén, J. Hagman, J. K. Jonasson, H. Deschout, D. Bernin, F. Cella-Zanacchi, A. Diaspro, J. G. McNally, M. Ameloot, N. Smisdom, M. Nydén, A. M. Hermansson, M. Rudemo, K. Braeckmans, *Q. Rev. Biophys.* **2015**, *48*, 323.